Received: 5 July 2019 | Revised: 28 October 2019 | Accepted: 10 December 2019

DOI: 10.1002/mgg3.1100

ORIGINAL ARTICLE

Molecular Genetics & Genomic Medicine Open Access WILEY

A novel de novo nonsense mutation in *ZC4H2* causes Wieacker-Wolff Syndrome

Dan Wang[1] | **Dongjie Hu**[1] | **Zhichao Guo**[2] | **Rong Hu**[1] | **Qunxian Wang**[1] | **Yannan Liu**[1] | **Mingjing Liu**[1] | **Zijun Meng**[1] | **Huan Yang**[1] | **Yun Zhang**[3] | **Fang Cai**[3] | **Weihui Zhou**[1] | **Weihong Song**[1,3]

[1]Chongqing City Key Lab of Translational Medical Research in Cognitive Development and Learning and Memory Disorders, and Ministry of Education Key Lab of Child Development and Disorders, Children's Hospital of Chongqing Medical University, Chongqing, China

[2]Department of Internal Neurology, Children's Hospital of Chongqing Medical University, Chongqing, China

[3]Townsend Family Laboratories, Department of Psychiatry, The University of British Columbia, Vancouver, BC, Canada

Correspondence
Weihong Song, Department of Psychiatry, The University of British Columbia, Vancouver, Canada.
Email: weihong@mail.ubc.ca

Funding information
Canada Research Chairs, Grant/Award Number: Canada Research Chair in Alzheimer's Disease

Abstract

Background: Wieacker-Wolff syndrome (WWS) is a congenital X-linked neuromuscular disorder, which was firstly reported in 1985. Zinc finger C4H2-type containing (*ZC4H2*) gene has been found to be associated with the disease pathogenesis. However, the underlying mechanism remains elusive.

Methods: Whole-exome sequencing was performed to identify the mutations. Expression plasmids were constructed and cell culture and immune-biochemical assays were used to examine the effects of the mutation.

Results: We reported a female patient with classical symptoms of WWS and discovered a novel nonsense heterozygous mutation (p.R67X; c.199C>T) in *ZC4H2* gene in the patient but not in her parents. The mutation resulted in a 66 amino-acid truncated ZC4H2 protein. The mutation is located in the key helix domain and it altered the subcellular locations of the mutant ZC4H2 protein. X-chromosome inactivation (XCI) pattern analysis revealed that the XCI ratio of the proband was 22:78.

Conclusion: Female heterozygous carriers with nonsense mutation with a truncated ZC4H2 protein could lead to the pathogenesis of Wieacker-Wolff syndrome and our study provides a potential new target for the disease treatment.

KEYWORDS

Arthrogryposis multiplex congenita, nonsense mutation, Wieacker-Wolff syndrome, X-chromosome inactivation, ZC4H2

1 | INTRODUCTION

Arthrogryposis multiplex congenita (AMC) is a rare neuromuscular syndrome with an incidence of one in 3000–5000 live births (Lowry, Sibbald, Bedard, & Hall, 2010). AMC is characterized by contracted muscles and nonprogressive congenital contractures of at least two different joints with thick periarticular capsules (Bamshad, Van Heest, & Pleasure, 2009; Hall, 2013). However, the mechanism underlying its pathogenesis is still unclear (Hall, 2012, 2014). As a heterogeneous disorder, AMC could be a single-gene disorder or sporadic without known genetic defect.

Dan Wang and Dongjie Hu contributed equally to this work.

Currently, over 300 genes are associated with AMC, among which 50 are X-linked (Bayram et al., 2016; Hall, 2014; Hall & Kiefer, 2016; Hunter et al., 2015; Michalk et al., 2008). In 1985, Wieacker et al reported 6 males in a family suffering from a syndrome with multiple congenital contractures, slowly progressive distal muscular atrophy, ocular movement disorder, and mild intellectual disability (ID) (Wieacker et al., 1985). The syndrome was then named after him as Wieacker-Wolff syndrome (WWS). WWS is a rare intellectual and developmental disability (IDD) disease. As a severe X-linked neurodevelopmental disorder with arthrogryposis, mutations in the *ZC4H2* (Zinc Finger C4H2-Type Containing) gene were identified to associate with WWS in 5 families and 3 sporadic cases with AMC and ID (Hirata et al., 2013). The male patients have more severe symptoms than female as the disease had been originally identified to be X-linked recessive inheritance (Hirata et al., 2013; Wieacker et al., 1985). However, female patients show various symptoms especially in deletion and nonsense mutation cases, and some of them are considered to be associated with nonrandom X-chromosome inactivation (XCI) (Hirata et al., 2013). So far, 7 missense mutations, 1 nonsense mutation, 1 frameshift mutation, 1 chromosomal breakpoint in Xq11.2, and 4 deletions in *ZC4H2* gene have been reported (Figure 1) (Godfrey, Dowlatshahi, Martin, & Rothkopf, 2018; Hennekam, Barth, Van Lookeren Campagne, De Visser, & Dingemans, 1991; Hirata et al., 2013; Kondo et al., 2018; May et al., 2015; Okubo et al., 2018; Zanzottera et al., 2017). The clinical presentation and genetic changes in female patients have been summarized in Table 1.

The human *ZC4H2* gene is located on the long arm of the X chromosome (Xq11.2) with 5 exons and encodes a member of the zinc finger domain-containing protein family. Its C-terminus has a typical zinc finger domain with four cysteine residues and two histidine residues. The expression of ZC4H2 is highest during embryonic development as well as immature neurons, and declined postnatally as well as in mature neurons, indicating its important role in the development of the nervous system (Hirata et al., 2013). *ZC4H2* has been considered as a potential candidate gene for X-linked cognitive disability. Homozygous ZC4H2 mutant results in abnormal swimming capacity, pectoral fin flexion, and eye position in zebrafish (May et al., 2015). These findings are consistent with contractures and exotropia observed in patients with ZC4H2 mutations.

In this study, we identified a novel mutation in *ZC4H2* gene in a female patient suffering from Wieacker-Wolff syndrome. We investigated the XCI pattern of this patient and subcellular location of the truncated ZC4H2 protein. Our study provided novel insights into ZC4H2's role in the pathogenesis of Wieacker-Wolff syndrome.

2 | MATERIALS AND METHODS

2.1 | Ethical approval

All samples were collected after the couple had given their written informed consent, and the study was approved by the research ethical committee of the Children's Hospital of Chongqing Medical University.

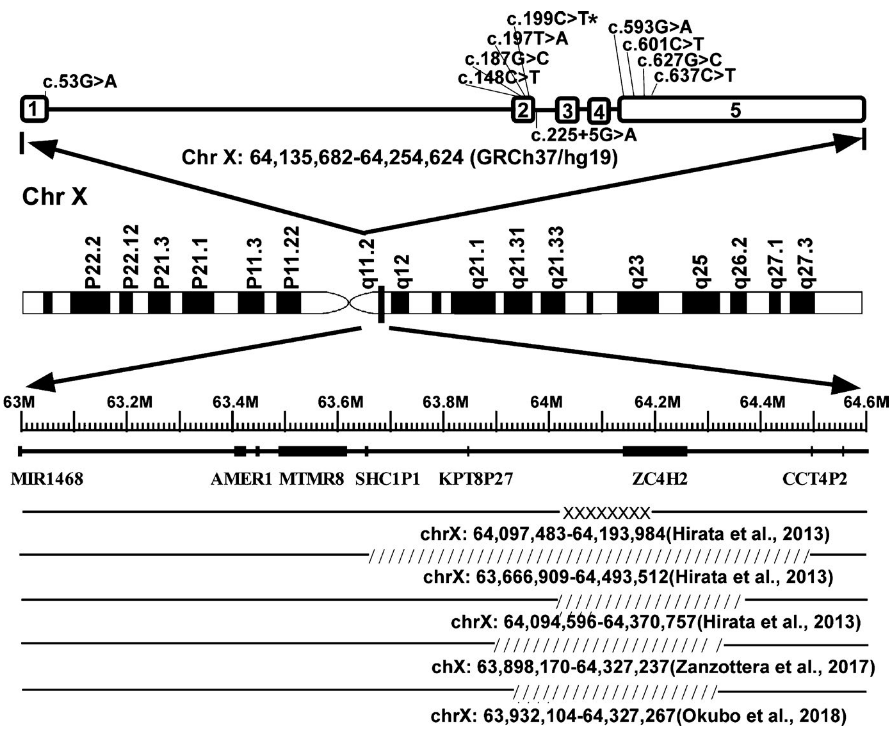

FIGURE 1 Schematic diagram of ZC4H2 with mutations. The structure of the human *ZC4H2* gene is schematically represented. All known mutations are shown at the top of the picture, while the position where the chromosome is deleted or inverted is shown at the bottom of the figure. Nucleotide numbering designates the A of the translation start codon ATG as +1. The numbered boxes represent exon. The "/"sign stands for deletion, while "×"signs shows the break point area."*" (c.199C>T) indicates the patient in the present study

TABLE 1 Comparison of physical presentation of female cases with ZC4H2 mutations

	Family 1	Family 2	Family 3	Family 4	Family 5	Family 6	Family 7	Family 8	Family 9	Simplex case 1	Simplex case 2	Simplex case 3	Simplex case 4	Simplex 5	Present case
mutation	c.593G>A (p.R198Q)	c.601C>T (p.P201S)	c.637C>T (p.R213W)	c.637C>T (p.R213W)	c.197T>A (p.L66H)	c.637C>T (p.R213W)	in-frame insertion: c.225+5G>A (p.V75in15aa)	c.53G>A (p.R18K)	c.627G>C (p.K209N)	Gene deletion: 63,666, 909-64,493, 512	Gene deletion: 64,049, 596-64,370, 757	Gene deletion: 63,898, 170-64,327, 237	Gene deletion: 63,932, 104-64,327, 267	c.148C>T (p.Q50X)	c.199C>T (p.R67X)
First author	Hirata et al. (2013)	Hennekam et al. (1991)	Hirata et al. (2013)	Hirata et al. (2013)	Miles& Carpenter (1991)	May et al. (2015)	May et al. (2015)	May et al. (2015)	Kondo et al. (2018)	Hirata et al. (2013)	Hirata et al. (2013)	Zanzottera et al. (2017)	Okubo et al. (2018)	Godfrey et al. (2018)	
Affected individuals	6	12	3	4	10	7	6	8	3	1	1	1	1	1	1
Affected females	1	7	1	2	6	4	3	4	1	1	1	1	1	1	1
XCI pattern	Skewed	Skewed	Normal	NA	Skewed	95:5/97:3	57:48	91:9	NA	Skewed	Skewed	Normal	NA	24:76	22:78
Short neck	–	1	–	–	–	–	–	–	–	–	1	–	1	–	1
High arched palate	–	1	–	–	2	–	–	–	–	–	1	–	–	–	1
Radial deviation of fingers	–	–	–	–	–	–	–	–	–	–	1	1	–	1	1
Ulnar deviation of fingers	–	1	–	–	–	–	–	–	–	–	–	1	–	1	
Camptodactyly	–	5	–	–	3	–	–	–	1	1	1	–	–	–	1
Proximally placed thumbs	–	–	–	–	4	–	–	–	–	–	1	–	–	–	1
Short toes	–	1	–	–	1	–	–	–	–	–	–	–	–	–	
Hip dislocation or contractures	–	1	–	–	1	–	–	–	–	–	1	1	1	1	1
Kyphosis, lordosis, or scoliosis	–	3	–	–	2	–	–	–	–	–	1	1	1	–	1
Talipes equinus	1	3	–	–	1	–	–	–	–	1	1	1	1	–	1
Intellectual disability	–	3	1	2	2	2	1	1	–	3	1	1	1	1	1
Seizures	–	–	–	–	–	1	1	–	–	–	–	–	–	–	–
MRI	–	–	–	–	–	–	–	–	–	–	–	Slight ventricular enlargement	Progressive diffuse cerebral atrophy	–	Normal
NCV	–	–	–	–	–	–	–	–	–	–	–	Normal	Normal	–	–

(Continues)

TABLE 1 (Continued)

	Family 1	Family 2	Family 3	Family 4	Family 5	Family 6	Family 7	Family 8	Family 9	Simplex case 1	Simplex case 2	Simplex case 3	Simplex case 4	Simplex 5	Present case
BAEP	–	–	–	–	–	–	–	–	–	–	–	–	Only waves I and II as normal latencies at 102dB	–	Wave I, III and V increased latency responses of the right and left ears at 80dB and 90dB respectivel-y
EEG	–	–	–	–	–	–	–	–	–	–	–	Occasional focal epileptic abnor-malities in both hemi-spheres	No epileptic discharges, but disor-ganiz-ed theta range activities	–	Normal

2.2 | Whole-exome sequencing

Coding exons were captured using the GenCap Liquid Phase Capture Kit (MyGenostics Inc) and sequenced on the Illumina NextSeq 500. Bcl2fastq conversion software was used for image analysis and base calling. Exome data processing, variant calling, and variant annotation were performed using BWA + GATK + ANNOVAR. Sequenced data were mapped to the genome assembly UCSC hg19 human reference genome. Single-nucleotide variations and small indels were identified using the HaplotypeCaller in GATK software. Variant sequences were filtered using VariantFiltration in GATK software. Filter-passed variants were annotated with ANNOVAR software.

2.3 | Plasmids

ZC4H2 (NM_018684) Human Tagged ORF Clone with C-terminal Flag tag (RC202589) was purchased from Origene. The R67X mutation (c.199C>T, p. R67X) was generated by using the QuikChange Lightning Site-Directed Mutagenesis Kit (Stratagene) with following primers: forward, CATGTGGAGGAACTCTGACTGATCCACGCTG; reverse, CAGCGTGGATCAGTCAGAGTTCCTCCACATG. To tag EGFP to the N-terminus of the ZC4H2 protein, ZC4H2 cDNA was subcloned into pEGFP-C2 vector at XhoI/BamHI sites. The primers used for cloning EGFP-ZC4H2 cDNA were as follows: forward 5′-CCGCTCGAGCATGGCAGATGA GCAAGAAA-3′; reverse 5′-CGCGGATCCTTATTCATCC TGCTTCCGT-3′. The clones were determined by restriction enzyme digestion followed by agarose gel electrophoresis, and the sequences were further confirmed by Sanger sequencing.

2.4 | Cell culture and immunoblot analysis

HEK293T cells were grown in Dulbecco's Modified Eagle Medium supplemented with 10% fetal bovine serum, penicillin (100 units/ml), and streptomycin (100 μg/ml) at 37°C with 5% CO2 until 95% confluence was attained.

A total of 5×10^5 HEK293T cells were grown in 6-well plates, and 4 μg of plasmid DNA was transfected using Lipofectamine2000 (Invitrogen) according to the manufacturer's recommendations. For Western blot analysis (Zhang et al., 2018), twenty-four hours later, the cells were lysed in RIPA buffer supplemented with the protease inhibitor cocktail (Roche Diagnostics), sonicated and centrifuged for 10 min at 12,000 rpm at 4°C. The samples were boiled after being diluted in 5 × SDS sample buffer, and equal quantities of total protein per lane were separated on 15% Tris-glycine-SDS-PAGE followed by transfer to polyvinylidene fluoride (PVDF-FL) membranes. Immunoblots were incubated with the following primary and secondary antibodies: rabbit polyclonal anti-ZC4H2 (1:1,000; Thermo Fisher), rabbit polyclonal anti-GFP (1:1,000; Beyotime).

2.5 | Confocal fluorescent microscopic analysis

HEK293T cells were plated on 20 mm diameter glass coverslips in 12-well plates and transfected using 0.2% Lipofectamine2000 (Invitrogen) with 2 μg wild type or mutant ZC4H2. After 24 hr of transfection, the cells were fixed with 4% paraformaldehyde for 20 min and permeabilized in 0.5% Triton X-100 for 30 min and then stained with ActinStain™ 555 phalloidin (CST) and DAPI.

2.6 | X-chromosome inactivation (XCI) assay

Genomic DNA Purification Kit (Promega) was used to extract human genomic DNA from peripheral blood leukocytes. XCI analysis was performed using well-characterized CpG methylation sites and polymorphic CAG repeats in exon 1 of androgen receptor (AR), according to the standard protocol (Allen, Zoghbi, Moseley, Rosenblatt, & Belmont, 1992). The ratio of shorter allele to longer allele was determined by methylation-sensitive restriction enzyme HpaII digestion followed by PCR amplification.

3 | RESULTS

3.1 | Case report

This patient is the first child of healthy nonconsanguineous parents of Chinese origin. She was born at term by scheduled cesarean section delivery due to breech presentation. Her birth weight (BW) was 3,150 g (25th-50th percentile), birth length (BL) 47.5 cm (10th-25th percentile), and occipito-frontal circumference (OFC) was 34.3 cm (50th percentile). The total Apgar (Appearance, Pulse, Grimace, Activity, and Respiration) score was 8, 10 and 10 at 1, 5, and 10 min after birth, respectively. Physical examination at birth demonstrated AMC and congenital developmental

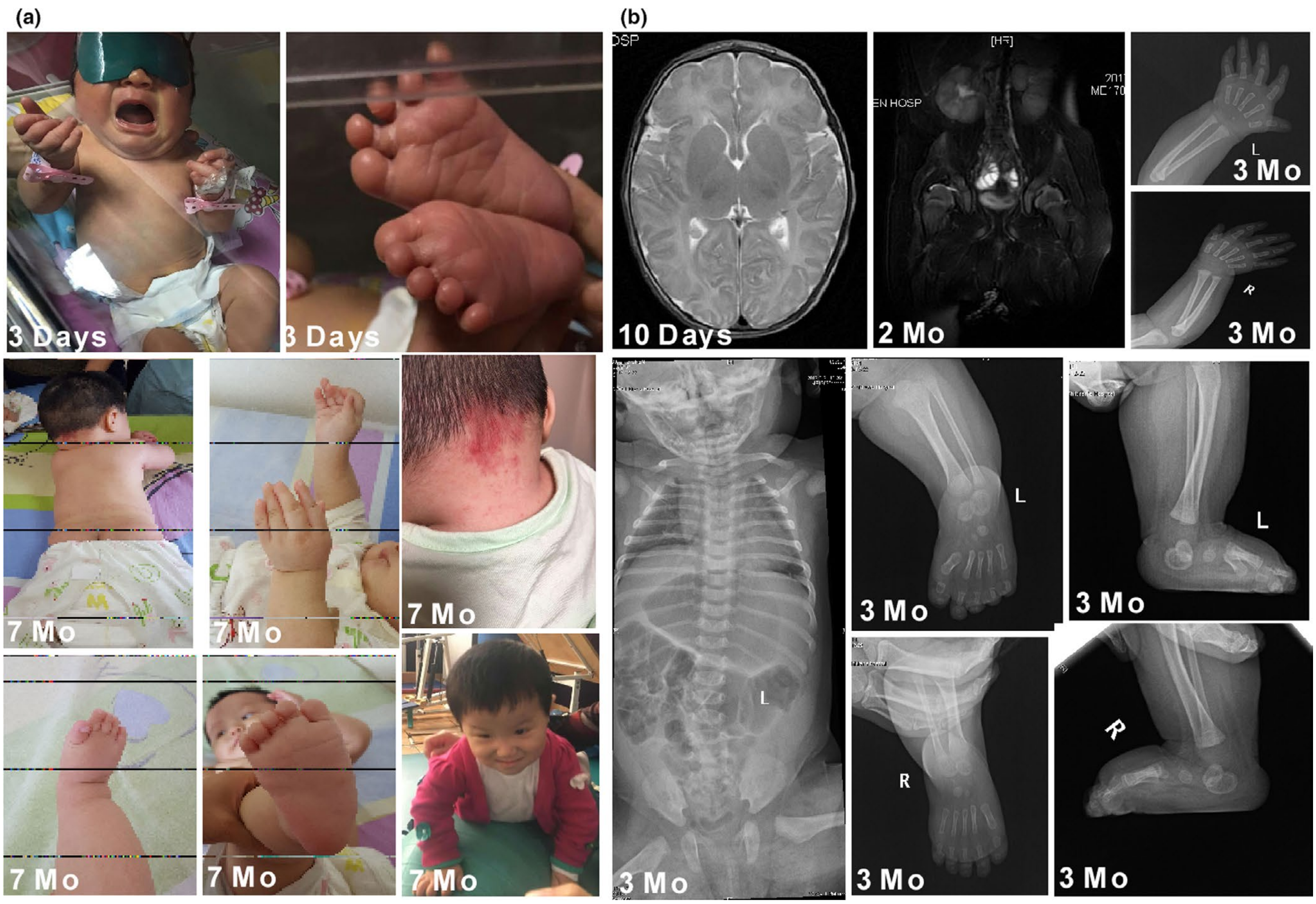

FIGURE 2 Clinical features of the female patient. (a) Images of the patient at 3 days, 7 months, and 22 months after birth showed overlapping and camptodactyly of fingers, right club foot, short neck, narrow shoulder, and short toes. (b) At 10 days, brain MRI is normal, pelvic MRI at 2 months showed right hip dislocation, and X-ray of limb at 3 months shows fixed contractures of fingers and vertical talus

malformation (Figure 2a). Cranial MRI and chest X-ray were normal, but echocardiography showed foramen ovale and the newborn hearing screening test was unsuccessful. Karyotype analysis and electroencephalogram were normal. At 45 days, her weight, length and OFC grew to 4,150 g, 51.5 cm, and 34.3 cm, respectively. At 2 months, a hip joint MRI indicated right developmental dysplasia of the hip (Figure 2b). At 3 months, brainstem auditory evoked potential (BAEP) showed the increased wave I, III, and V latency responses of the right and left ears at 80 and 90 dB, respectively. General movement assessment revealed mildly abnormal general movements. Electroencephalogram was normal. X-rays of the spine, hand and foot showed waist scoliosis, camptodactyly of the fingers, extorsion of the hands, and vertical talus. Since then, she has received rehabilitation training at a local healthcare center. At 3 months of age, she was taken to our hospital because of global developmental delay. During physical examination, she could not control her head and presented with truncal hypotonia as well as AMC. She also presented with flat nose; short neck; high, narrow palate, and short toes (Figure 2a). The Gesell Infant Development Scale (GESELL) (Chinese edition) test showed gross motor skills (GM) 11, fine motor skills (FM) 28, adaptability (AD) 39, language (L) 50, and personal social activity (PS) 50. Her fine and gross motor abilities were 1 + month and 0–1 month. Brain MRI and chest X-ray were normal. At 22 months of age, she could sit for a while and hold a bottle and drink milk by herself. When her parents put a biscuit in her hands, she was able to put it in her mouth slowly. She could not stand, and imaging examination showed osteonecrosis of the femoral head. The patient presents a typical WWS case.

3.2 | Next-generation sequencing identifies nonsense mutations in ZC4H2

To identify the pathogenic mutations in this patient, whole-exome sequencing (WES) followed by Sanger sequencing was performed on the blood DNA samples of the proband and her parents (Figure 3a). We identified a heterozygous nonsense mutation in the *ZC4H2* gene (c.199C>T, p. R67X) in this patient but not in her father and mother, indicating that the patient has a de novo mutation (Figure 3b). This mutation creates a new stop codon at amino acid residue 67 of ZC4H2 protein, resulting in a truncated ZC4H2 protein with 66 amino acids

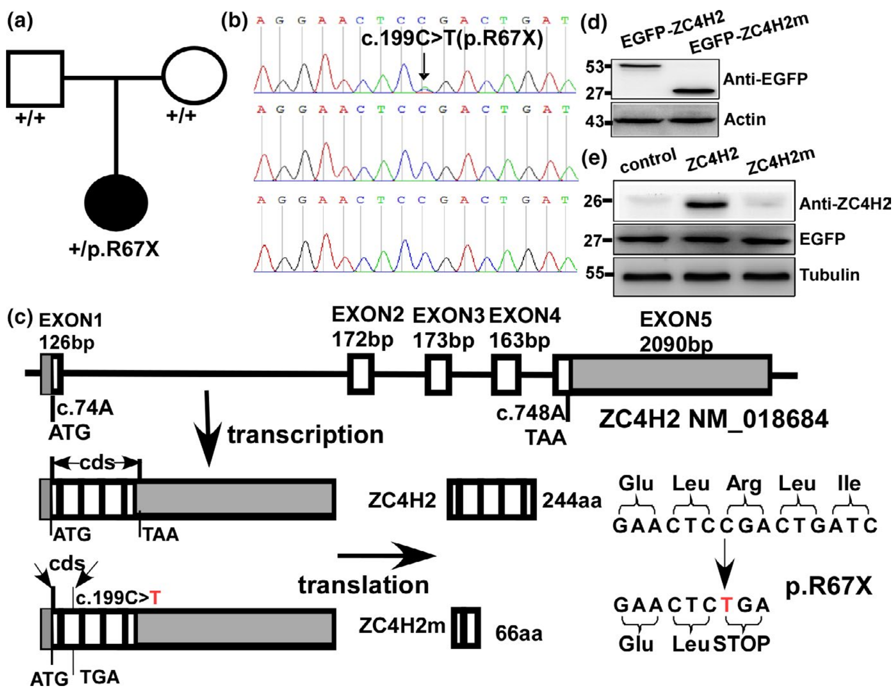

FIGURE 3 Identification of a de novo nonsense mutation R67X in *ZC4H2* gene. (a) Pedigree of the patient with ZC4H2 p.R67X mutation. (b) Sanger sequencing of *ZC4H2* gene in genomic DNA from the proband and her father and mother. The c.199C>T (p. R67X) was found in the patient but not in her parents, suggesting that the mutation was de novo. (c) Schematic diagram of ZC4H2 gene structure with mRNA and protein products. Wild type and mutant ZC4H2 coding sequences surrounding the mutation were shown. (d) HEK293T cells were transfected with plasmids expressing either N-terminal EGFP-tagged wild-type ZC4H2 or R67X mutant ZC4H2m. Anti-GFP antibody was used to detect the N-terminal EGFP-tagged proteins by Western blot using 15%Tris-Glycine SDS-PAGE gel. β-actin or β-tubulin was used as control. (e) HEK293T cells were transiently transfected with plasmids expressing either empty vector, or C-terminal Flag-tagged wild-type ZC4H2 and R67X mutant ZC4H2m. EGFP expression plasmid was co-transfected for transfection efficiency control. Anti-ZC4H2 antibody was used to detect the wildtype ZC4H2 protein. EGFP and β-tubulin was used as control

and lacking the last 158 amino acids at the C-terminus (Figure 3c). The mammalian expression plasmids carrying wild-type ZC4H2 cDNA or the mutant ZC4H2-R67X were constructed and the proteins were fused with EGFP tag at N-terminus or with Flag tag at C-terminus. The plasmids were transfected into HEK293T cells, and Western blot analysis was performed to examine the expression of the fusion proteins with anti-EGFP antibody. The wild-type plasmid with N-terminal EGFP tag expressed full-length EGFP-ZC4H2 proteins, whereas the mutant plasmid expressed a shorter version of EGFP-truncated ZC4H2 proteins (Figure 3d). The results were further confirmed by expression of C-terminal Flag-fused ZC4H2 proteins. The wild-type plasmid with C-terminal Flag tag expressed full-length Flag-ZC4H2 proteins; in contrast, the mutant plasmid carries a stop codon between N-terminus of ZC4H2 and C-terminal Flag, resulting in failed identification of a Flag-fused protein (Figure 3e). These results clearly demonstrated that we have discovered a novel WWS-associated nonsense mutation in ZC4H2 gene that results in a truncated protein.

3.3 | Altered subcellular location of R67X mutant protein

ZC4H2 protein contains a putative nuclear localization signal (NLS) within amino acids 207 to 224 (KAKSRSRNPKKPKRKQDE). Mutations in this area, such as R213W and K209N, were identified to interrupt nuclear transport (Hirata et al., 2013; Kondo et al., 2018). To investigate whether the newly identified nonsense mutation that abolished the nuclear localization signal would affect the subcellular localization of the protein, EGFP was fused to the N-terminus of the wild type and mutant ZC4H2 protein. The wild type (Figure 4e-h) and mutant plasmids (Figure 4i-l) as well as EGFP control plasmid (Figure 4a-d) were transfected into HEK293T cells, and the EGFP signals in cytoplasmic compartment and nuclei were analyzed using confocal fluorescent microscope. The results showed that wild-type ZC4H2 had perinuclear and nuclear punctate pattern of EGFP signals in the cells (Figure 4e-h, m), but the truncated protein had no such clear punctate pattern (Figure 4i-l, m), indicating the mutant protein's trafficking was altered.

3.4 | XCI of *ZC4H2* gene in the patient

In 2013, in order to investigate whether *ZC4H2* gene is subjected to XCI, its expression in blood lymphocytes was measured. It has been found that different XCI patterns may lead to the various phenotypes of female patients who have the same mutation in *ZC4H2* gene (Hirata et al.,

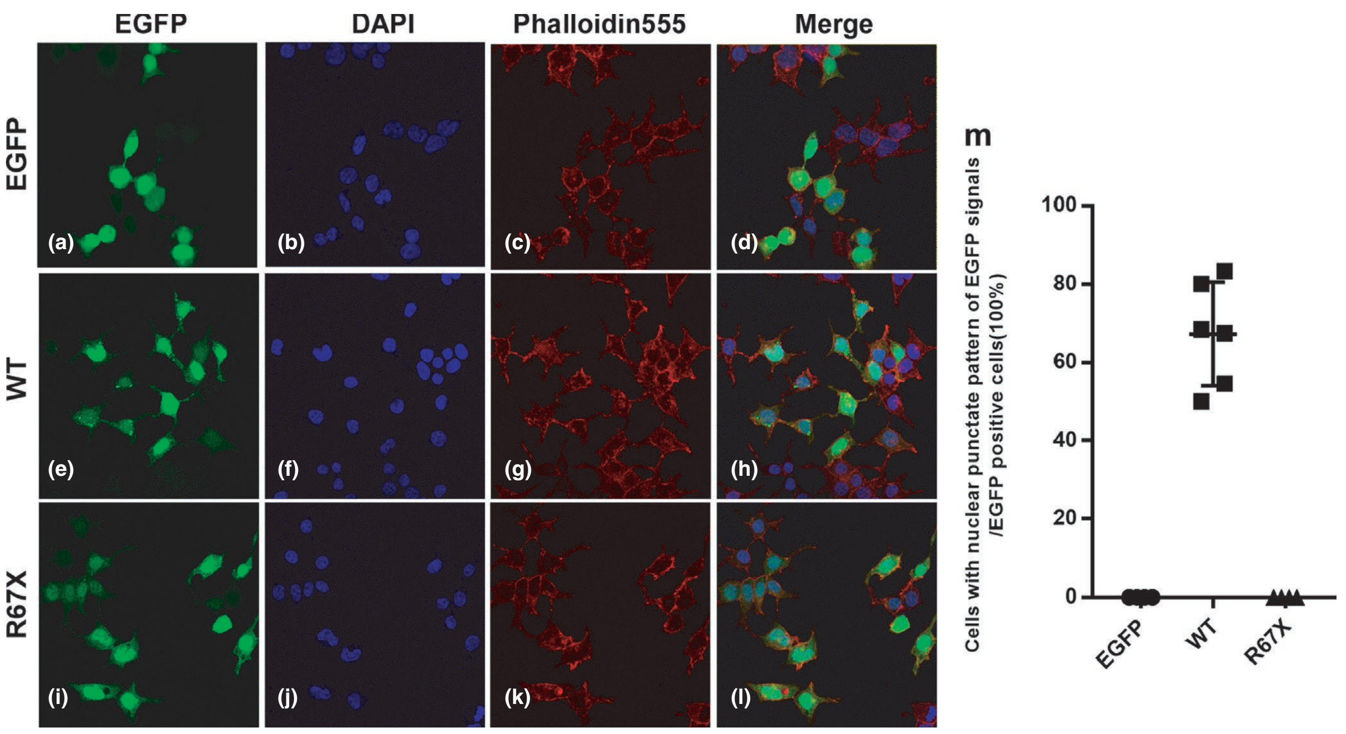

FIGURE 4 Confocal microscopic analysis. HEK293T cells were transfected with plasmids expressing either the wild-type ZC4H2 (e-h) or mutant ZC4H2 c.199 C>T (p. R67X) protein (i-l) with N-terminally tagged EGFP. The empty EGFP vector was used as the negative control (a-d). Phalloidin 555 and DAPI were used to stain the cytoskeleton and nucleus, respectively. Merged images of EGFP, DAPI, and phalloidin 555 are observed in d, h, and l. (m) An increased presence of wild-type N-EGFP-ZC4H2 protein punctuate aggregated in the cytosol while the truncated protein is in the cytosol and nuclei at the same time, similar to EGFP protein only

2013). However, other studies showed controversial results (May et al., 2015; Zanzottera et al., 2017). In order to confirm whether different XCI pattern is the cause of the serious phenotype of the female patient, we also extracted the patient's peripheral blood and performed XCI analysis. The assessment of the XCI pattern showed a ratio of 22:78 (Figure 5), this random inactivation pattern further confirmed the hypothesis May et al. and Zanzottera et al. concluded in their study (May et al., 2015; Zanzottera et al., 2017), in which they found there was no significant correlation between XCI patterns and disease phenotypes, suggesting that there are other reasons to participate and requires further research.

4 | DISCUSSION

In 1985, Wieacker-Wolff firstly described a family with 6 males, who had club feet, progressive distal muscular atrophy, oculomotor apraxia, dysarthria, and IDD. The

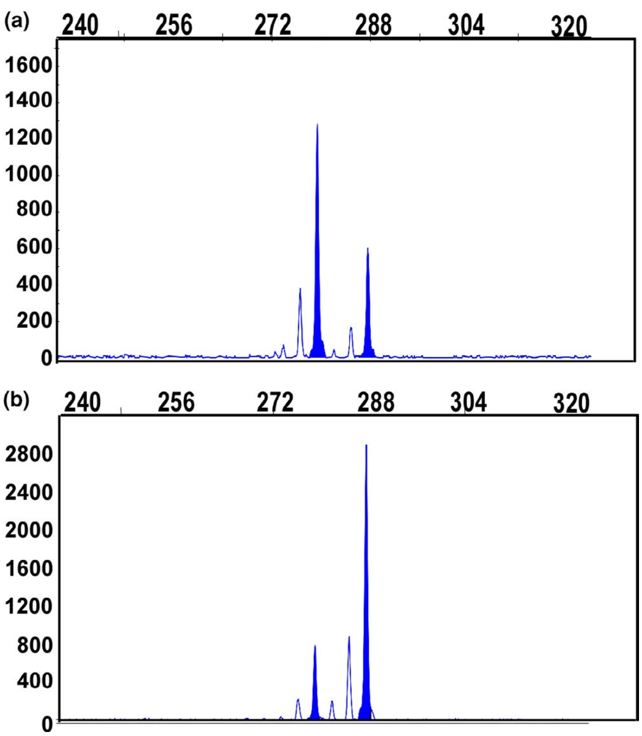

FIGURE 5 X-chromosome inactivation analysis of the patient with the R67X ZC4H2 mutation (proband). Amplification peaks of the smaller and larger CAG repeat alleles of the androgen receptor gene before (a) and after (b) digestion with the enzyme HhaI. The *Y*-axis shows the amplification peak values corresponding to the number of PCR products of each allele. The amplification values of the smaller size allele (279 bp), undigested and digested, were 1,286 and 782, respectively. For the larger size allele (287 bp), undigested and digested amplification values were 605 and 2,884, respectively. The calculated X-chromosome inactivation ratio was 22:78 according to the method described before

syndrome with muscular atrophy was considered to be neurogenic. The family also had 12 healthy males and 22 females, suggesting that the pedigree is consistent with X-linked recessive inheritance. However, the etiology was not clear until Kloos et al mapped the genetic defect to Xp11.3 ± 11.3 in 1997 (Kloos, Jakubiczka, Wienker, Wolff, & Wieacker, 1997). ZC4H2 mutations were identified as the cause of the disease (Hirata et al., 2013). There have been 7 missense mutations identified in 9 families, 1 chromosomal inversion caused by breakpoint in Xq11.2, 1 frameshift mutation, 2 nonsense mutations, and 4 deletions in sporadic cases (Figure 1).

AMC may be an endophenotype of more than 400 disorders, 50 of which are identified to be X-linked. Wieacker-Wolff Syndrome has been considered as a disorder with X-linked recessive inheritance (Wieacker et al., 1985). However, females with heterozygous *ZC4H2* mutations found in 4 of 5 families and 2 sporadic cases were developed the symptoms including equinovarus feet and mild ID. In this study, the author also found that women carrying the same mutations may have different phenotypes and suggested that nonrandom XCI might be responsible for this phenomenon (Hirata et al., 2013). However, it was found that even in female patients with the same mutation and similar phenotypes, their XCI was varied (May et al., 2015). A female patient with a severe phenotype caused by a small heterozygous deletion of the *ZC4H2* gene at Xq11.2 and a female with a mild phenotype caused by a p.Q50X nonsense mutation showed randomized X inactivation. These results indicate that there is no strong correlation between X inactivation and disease phenotype. The proband patient in our current study carrying a nonsense mutation (p.R67X) for a truncated protein with a more serious phenotype showed an XCI ratio of 22:78, which also suggests that X inactivation could not account for the phenotypic discrepancy in the ZC4H2 mutations-associated WWS female patients. It is likely that the ZC4H2 deletion or nonsense mutations have a stronger detrimental effect on ZC4H2 function that leads to WWS in heterozygous female carriers while these mutations would be lethal to males. The data may suggest that a partial loss of ZC4H2 protein function may be enough to trigger the pathogenesis of WWS. This does not rule out the truncated protein could have abnormal gain of function to lead to WWS pathogenesis. Using the I-TASSER program to analyze ZC4H2 protein's structure and function (Roy, Kucukural, & Zhang, 2010; Wang, Virtanen, Xue, & Zhang, 2017; Yang & Zhang, 2015), all reported mutations were located in the first helix and last coiled-coil region (Figure 6), suggesting that the helix and coil domain may be essential for its function.

In summary, we identified a novel nonsense mutation in *ZC4H2* gene in a female patient suffering from severe Wieacker-Wolff syndrome and this mutation results in a truncated ZC4H2 protein. We have shown the mutation affects the protein's trafficking and XCI might not be responsible for its detrimental effect. The results suggest that female

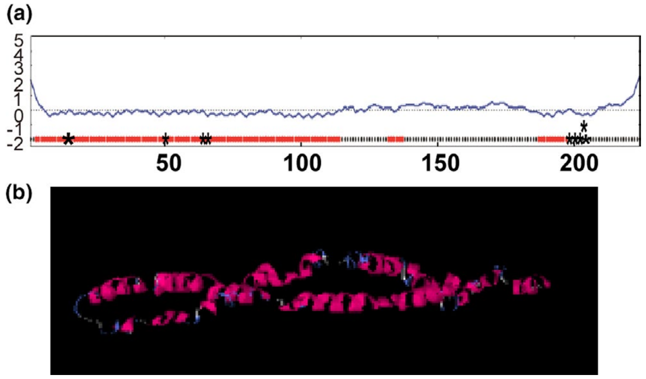

FIGURE 6 Protein structure by I-TASSER modeling. (a) The secondary structural of ZC4H2 protein, helix are shown in red, and the coil is in black. " * " represents the previous reported pointed, nonsense and frameshift mutations, and the present mutation is shown in blue " * ". (b) The 3-dimensional atomic model based on the protein sequence generated by the iterative threading assembly refinement server

heterozygous carriers with loss of or a truncated ZC4H2 protein could also lead to the pathogenesis of Wieacker-Wolff syndrome. Further study is warranted to define this mutation's effect on ZC4H2's function and its role in the pathogenesis of Wieacker-Wolff syndrome.

ACKNOWLEDGMENTS

We thank the patients and her parents for participating in this study. We also thank Bin Tan for experimental assistance with confocal microscopy. WS is the holder of the Tier 1 Canada Research Chair in Alzheimer's Disease.

CONFLICT OF INTEREST

The authors declare that they have no competing financial interests.

AUTHOR CONTRIBUTION

DW and WS conceived and designed the experiments; DW and DH performed the experiments; DW, DH, ZG, RH, QW, YL, ML, ZM, HY, YZ, FC, WZ, and WS analyzed and contributed reagents/materials/analysis tools; DW, YZ, FC, and WS wrote the paper. All authors reviewed the manuscript.

DATA AVAILABILITY STATEMENT

The data that support the findings of this study are available from the corresponding author upon reasonable request.

ORCID

Weihong Song https://orcid.org/0000-0001-9928-889X

REFERENCES

Allen, R. C., Zoghbi, H. Y., Moseley, A. B., Rosenblatt, H. M., & Belmont, J. W. (1992). Methylation of HpaII and HhaI sites near the polymorphic CAG repeat in the human androgen-receptor gene correlates with X chromosome inactivation. *American Journal of Human Genetics*, *51*(6), 1229–1239.

Bamshad, M., Van Heest, A. E., & Pleasure, D. (2009). Arthrogryposis: A review and update. *Journal of Bone and Joint Surgery. American Volume*, *91*(Suppl 4), 40–46. https://doi.org/10.2106/JBJS.I.00281

Bayram, Y., Karaca, E., Coban Akdemir, Z., Yilmaz, E. O., Tayfun, G. A., Aydin, H., … Lupski, J. R. (2016). Molecular etiology of arthrogryposis in multiple families of mostly Turkish origin. *J Clin Invest*, *126*(2), 762–778. https://doi.org/10.1172/JCI84457

Godfrey, N. D., Dowlatshahi, S., Martin, M. M., & Rothkopf, D. M. (2018). Wieacker-Wolff syndrome with associated cleft palate in a female case. *American Journal of Medical Genetics. Part A*, *176*(1), 167–170. https://doi.org/10.1002/ajmg.a.38527

Hall, J. G. (2012). Arthrogryposis (multiple congenital contractures) associated with failed termination of pregnancy. *American Journal of Medical Genetics Part A*, *158A*(9), 2214–2220. https://doi.org/10.1002/ajmg.a.35531

Hall, J. G. (2013). Arthrogryposes (Multiple Congenital Contractures). In D. Rimoin, R. Pyeritz, & B. Korf (Eds.), *Emery and Rimoin's Principles and Practice of Medical Genetics* (Chapter 2, pp. 1–101). Philadelphia, PA: Elsevier Ltd.

Hall, J. G. (2014). Arthrogryposis (multiple congenital contractures): Diagnostic approach to etiology, classification, genetics, and general principles. *European Journal of Medical Genetics*, *57*(8), 464–472. https://doi.org/10.1016/j.ejmg.2014.03.008

Hall, J. G., & Kiefer, J. (2016). Arthrogryposis as a syndrome: Gene ontology analysis. *Molecular Syndromology*, *7*(3), 101–109. https://doi.org/10.1159/000446617

Hennekam, R. C., Barth, P. G., Van Lookeren Campagne, W., De Visser, M., & Dingemans, K. P. (1991). A family with severe X-linked arthrogryposis. *European Journal of Pediatrics*, *150*(9), 656–660. https://doi.org/10.1007/BF02072628

Hirata, H., Nanda, I., van Riesen, A., McMichael, G., Hu, H., Hambrock, M., … Kalscheuer, V. M. (2013). ZC4H2 mutations are associated with arthrogryposis multiplex congenita and intellectual disability through impairment of central and peripheral synaptic plasticity. *American Journal of Human Genetics*, *92*(5), 681–695. https://doi.org/10.1016/j.ajhg.2013.03.021

Hunter, J. M., Kiefer, J., Balak, C. D., Jooma, S., Ahearn, M. E., Hall, J. G., & Baumbach-Reardon, L. (2015). Review of X-linked syndromes with arthrogryposis or early contractures-aid to diagnosis and pathway identification. *American Journal of Medical Genetics. Part A*, *167A*(5), 931–973. https://doi.org/10.1002/ajmg.a.36934

Kloos, D. U., Jakubiczka, S., Wienker, T., Wolff, G., & Wieacker, P. (1997). Localization of the gene for Wieacker-Wolff syndrome in the pericentromeric region of the X chromosome. *Human Genetics*, *100*(3–4), 426–430. https://doi.org/10.1007/s004390050528

Kondo, D., Noguchi, A., Takahashi, I., Kubota, H., Yano, T., Sato, Y., … Takahashi, T. (2018). A novel ZC4H2 gene mutation, K209N, in Japanese siblings with arthrogryposis multiplex congenita and intellectual disability: Characterization of the K209N mutation and clinical findings. *Brain Dev*, *40*(9), 760–767. https://doi.org/10.1016/j.braindev.2018.05.003

Lowry, R. B., Sibbald, B., Bedard, T., & Hall, J. G. (2010). Prevalence of multiple congenital contractures including arthrogryposis multiplex congenita in Alberta, Canada, and a strategy for classification and coding. *Birth Defects Research Part A: Clinical *and Molecular Teratology*, *88*(12), 1057–1061. https://doi.org/10.1002/bdra.20738

May, M., Hwang, K. S., Miles, J., Williams, C., Niranjan, T., Kahler, S. G., … Kim, C. H. (2015). ZC4H2, an XLID gene, is required for the generation of a specific subset of CNS interneurons. *Human Molecular Genetics*, *24*(17), 4848–4861. https://doi.org/10.1093/hmg/ddv208

Michalk, A., Stricker, S., Becker, J., Rupps, R., Pantzar, T., Miertus, J., … Hoffmann, K. (2008). Acetylcholine receptor pathway mutations explain various fetal akinesia deformation sequence disorders. *American Journal of Human Genetics*, *82*(2), 464–476. https://doi.org/10.1016/j.ajhg.2007.11.006

Miles, J. H., & Carpenter, N. J. (1991). Unique X-linked mental retardation syndrome with fingertip arches and contractures linked to Xq21.31. *American Journal of Medical Genetics*, *38*, 215–223.

Okubo, Y., Endo, W., Inui, T., Suzuki-Muromoto, S., Miyabayashi, T., Togashi, N., … Haginoya, K. (2018). A severe female case of arthrogryposis multiplex congenita with brain atrophy, spastic quadriplegia and intellectual disability caused by ZC4H2 mutation. *Brain Dev*, *40*(4), 334–338. https://doi.org/10.1016/j.braindev.2017.11.011

Roy, A., Kucukural, A., & Zhang, Y. (2010). I-TASSER: A unified platform for automated protein structure and function prediction. *Nature Protocols*, *5*(4), 725–738. https://doi.org/10.1038/nprot.2010.5

Wang, Y., Virtanen, J., Xue, Z., & Zhang, Y. (2017). I-TASSER-MR: Automated molecular replacement for distant-homology proteins using iterative fragment assembly and progressive sequence truncation. *Nucleic Acids Research*, *45*(W1), W429–w434. https://doi.org/10.1093/nar/gkx349

Wieacker, P., Wolff, G., Wienker, T. F., Sauer, M., Opitz, J. M., & Reynolds, J. F. (1985). A new X-linked syndrome with muscle atrophy, congenital contractures, and oculomotor apraxia. *American Journal of Medical Genetics*, *20*(4), 597–606. https://doi.org/10.1002/ajmg.1320200405

Yang, J., & Zhang, Y. (2015). I-TASSER server: New development for protein structure and function predictions. *Nucleic Acids Research*, *43*(W1), W174–181. https://doi.org/10.1093/nar/gkv342

Zanzottera, C., Milani, D., Alfei, E., Rizzo, A., D'Arrigo, S., Esposito, S., & Pantaleoni, C. (2017). ZC4H2 deletions can cause severe phenotype in female carriers. *American Journal of Medical Genetics. Part A*, *173*(5), 1358–1363.

Zhang, S., Cai, F., Wu, Y., Bozorgmehr, T., Wang, Z., Zhang, S. I., … Song, W. (2018). A presenilin-1 mutation causes Alzheimer disease without affecting Notch signaling. *Molecular Psychiatry*, https://doi.org/10.1038/s41380-018-0101-x

How to cite this article: Wang D, Hu D, Guo Z, et al. A novel de novo nonsense mutation in *ZC4H2* causes Wieacker-Wolff Syndrome. *Mol Genet Genomic Med*. 2020;8:e1100. https://doi.org/10.1002/mgg3.1100